

Hyperbranched Intumescent Flame-Retardant Agent: Application to Natural Rubber Composites

Wang Jincheng, Guo Yan

College of Chemistry and Chemical Engineering, Shanghai University of Engineering Science, Shanghai 201620, China

Received 21 December 2010; accepted 26 February 2011

DOI 10.1002/app.34407

Published online 25 July 2011 in Wiley Online Library (wileyonlinelibrary.com).

ABSTRACT: The first part of this investigation focused on the synthesis and characterization of a hyperbranched intumescent flame-retardant (HIFR) agent. Two steps were used in the synthetic process. The structure was characterized by scanning electron microscopy (SEM), thermogravimetric analysis (TGA), and Fourier transform infrared spectroscopy (FTIR). The second part focused on the application of HIFR agent into natural rubber (NR) composites. The cure characteristics, tensile properties,

wear resistance, and flame-retardant property of HIFR/NR composites were evaluated. It was demonstrated that the addition of this HIFR agent into NR led to an improvement in its physicochemical and flame-retardant properties. © 2011 Wiley Periodicals, Inc. *J Appl Polym Sci* 122: 3474–3482, 2011

Key words: intumescent flame retardant; hyperbranched technology; natural rubber; characterization

INTRODUCTION

Natural rubber (NR) has some unique advantages over competitive synthetic rubbers such as properties required for special applications like manufacture of aerotires, suspension elements, and various latex products. Despite a number of superior qualities, one of the setbacks of NR that limits its usage for highly demanding applications such as coal mine conveyor belts, power cables, and aircraft tire treads is its inherently high flammability.¹

One way to decrease the flammability of polymer materials is to introduce a flame-retardant additive. The use of intumescent additives allows both fire properties and mechanical behavior of the materials to be optimized.^{2–4} An intumescent flame-retardant (IFR) system is usually used as combinations, and the typical example is the composite of ammonium-polyphosphate (APP), pentaerythritol (PER), and melamine (ME).⁵ The proposed mechanisms of an

IFR agent are based on the charred layer acting as a physical barrier, which slows down heat and mass transfer between the gas and condensed phases.⁶

However, intumescent formulations with IFR agents are unfortunately not permanent. Indeed, these agents have a poor compatibility with the polymeric materials. Thus, problems of migration and solubility may occur.

To overcome these problems, hyperbranched modification technology is now used. Hyperbranched macromolecules have porous and three-dimensional structure and have plenty of functional end groups. This can make them more reactive. For high degree of branched structure, they are difficult to crystallize and have higher compatibility with other polymers.⁷

In this work, we initially describe the preparation of IFR agent coated by a hyperbranched polymer using a two-step method. Then, the related structure and properties of the hyperbranched intumescent flame-retardant (HIFR) agent are characterized by scanning electron microscopy (SEM), thermogravimetric analysis (TGA), and Fourier transform infrared (FTIR) spectroscopy. However, other interest of this work is to study the physical and mechanical properties of the HIFR-filled NR composites including cure characteristics, tensile properties, flame retardance, and wear resistance.

EXPERIMENTAL

Materials

To prepare this new HIFR agent, APP ((NH₄PO₃)_n, H = 700, Hostamflam 422, Hoechst, soluble fraction

Correspondence to: G. Yan (guoyan618596@163.com).

Contract grant sponsor: "National Natural Science Funds; contract grant number: 50803034.

Contract grant sponsor: Shanghai Municipal Education Commission and Shanghai Education Development Foundation ("Shu Guang" project); contract grant number: 10SG53.

Contract grant sponsor: "Shanghai Nano-project Funds; contract grant number: 0952nm02600.

Contract grant sponsor: "Shanghai Universities Knowledge Innovation Engineering Project; contract grant number: JZ0904.

TABLE I
Formulation of NR Vulcanizates

Ingredients	Loading (phr)
NR	100
Sulfur	2.5
Zinc oxide	5.0
Stearic acid	1.0
2-benzothiazolethiol	1.2
Tetramethyl thiuram disulfide	0.2
Diphenyl guanidine	0.3
Electric insulating oil	8.0
Semireinforcing carbon black	30
IFR or HIFR	0/20/40/60/80

in H₂O: <1 wt %), pentaerythritol (PER; Aldrich), and melamine (ME) (Aldrich) were supplied by Shanghai Nanxiang Organic Plant (Shanghai, China) and were all used as received. Methyl acrylate, diethanolamine, methanol, and toluene-*p*-sulfonic acid were supplied by Shanghai Guoyao Chemical Company (Shanghai, China).

To compare the physical, mechanical, and flame-retardant properties between IFR/NR and HIFR/NR composites, following formulation, which was presented in Table I, is used. NR and 3# bacon rubber, industrial grade, are supplied by Shanghai Hongshun Co. (Shanghai, China). Semireinforcing carbon black, industrial grade, is supplied by Huangyan Zhedong Rubber Co. (Zhejiang, China). Sulfur and zinc oxide, chemical grade, are supplied by Shanghai Guoyao Chemical Group (Shanghai, China). Stearic acid, analytical grade, is supplied by Shanghai Lingfeng Chemical Agent Co. (Shanghai, China). 2-Benzothiazolethiol, tetramethyl thiuram disulfide, diphenyl guanidine, and electric insulating oil, chemical grade, are supplied by Shenyang Leshan Chemical Additive Co. (Liaoning, China).

Preparation of HIFR agent

The following two-step method was used to prepare the hyperbranched intumescent flame-retardant (HIFR) agents. The first step was to synthesize the monomer of hyperbranched polymer. About 0.1 mol of diethanolamine, 0.1 mol of methyl acrylate, and 10 mL of methanol were added into a three-necked flask provided with a stirrer. The mixtures were treated at 35°C for about 4 h at N₂ atmosphere. The product was separated by distillation until no methanol was remained. The product, methyl 3-[bis(2-hydroxyethyl)amino]propionate was obtained as stable transparent oil liquid. The density, refractive index, and boiling point were 1.04 g/cm³, 1.44, and 110°C, respectively. Yield: ~ 85%.

The second step was to prepare HIFR agents. A 250-mL four-necked flask with a mechanical stirrer, thermometer, and a tube with N₂ atmosphere was

used as a reactor. About 10 g of IFR agent (APP : PER : ME = 3 : 1 : 1, wt %) and 0.1 g of toluene-*p*-sulfonic acid (catalyst) were gradually added to 0.1 mol of a prior prepared solution of methyl 3-[bis(2-hydroxyethyl)amino] propionate. The resultant suspension was vigorously stirred for 10 h. The treated IFR agent was repeatedly washed. The filter cake was then placed in a vacuum oven at 80°C for 6 h for drying. The dried cake was ground to obtain the white HIFR powders. Yield: ~ 90%.

Preparation of NR composites

IFR/NR and HIFR/NR composites were prepared on a double roller plasticator, operating at 20°C. The sheeted compounds were conditioned at 20°C for 24 h before testing.

Characterization

FTIR spectroscopy

Fourier transform infrared (FTIR) spectra were recorded on a Nicolet 170SX Fourier transform infrared spectrophotometer (Nicolet Avatar 370) in the range 4000–600 cm⁻¹ at a resolution of 2 cm⁻¹. Samples were ground and mixed with KBr to form pellets. Sixty-four scans were necessary to obtain spectra with good signal-to-noise ratios.

Photos and SEM

The photos of the horizontal burning of these composites were taken by a digital Sony camera. Scanning electron microscopy (SEM) was observed using a Hitachi S-2150 scanning electron microscope. The SEM was taken using an electron beam potential of 25 kV. The samples were gold coated using an IB-3 Ionic sputtermeter.

FR tests

Limiting oxygen index (LOI) was measured using a Stanton Redcroft instrument on sheets (100 × 10 × 3 mm³) according to ASTM 2863.

Thermal analysis

TGA was carried out at 10°C/min under nitrogen (flow rate 5 × 10⁻⁷ m³/s) using a Linseis PT-1000 microbalance. In each case, the mass of samples used was fixed at 10 mg, and the samples (powder mixtures) were positioned in open vitreous silica pans. The precision of the temperature measurements was 1°C over the whole range of temperatures.

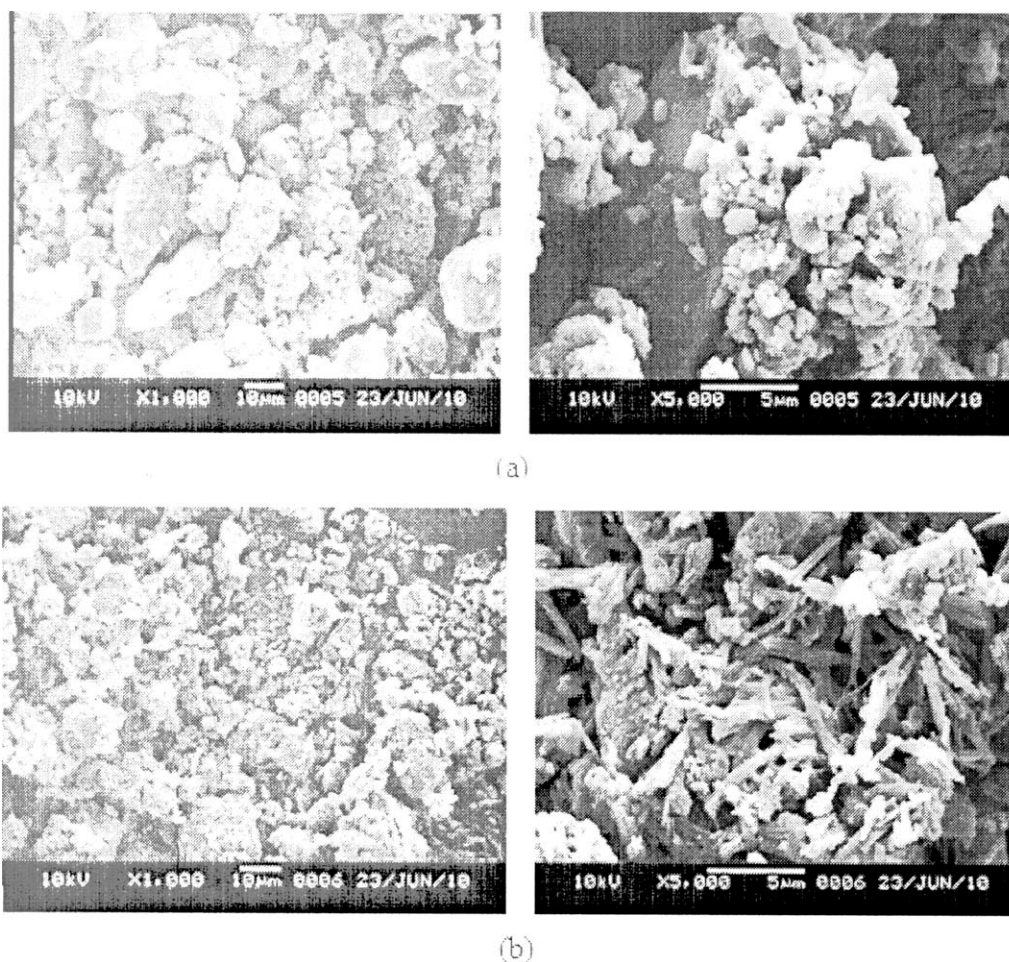


Figure 1 SEM of (a) IFR agent and (b) HIFR agent.

Mechanical properties

The curing parameters were determined on an oscillating disk rheometer (MDR-2000, Wuxi, Liyuan, China) according to ASTM D 2084-81. The compositions were then vulcanized at 150°C for 10 min during the optimum cure times under 15 MPa pressure on an electrically heated press. To compare test results conveniently, all the uncured mixes and vulcanizates in this work were prepared using the above conditions and the formulation shown in Table I except for the change of the amount of IFR or HIFR agent.

The tensile properties of the vulcanizates were measured with dumbbell specimens (6 mm wide in cross section) according to the Chinese National Standard GB 528-82. The value for each sample was taken as the median value of five specimens. These tests were carried out at room temperature on a universal tensile testing machine (TCS-2000, Dongguan, China), with a crosshead speed of 500 mm/min. The tensile specimens for each composition were tested, and the stress and strain at break were determined.

Shore hardness test was conducted using a XY-1 rubber hardness instrument.

The wear-resistant tests of the vulcanized rubber composites were conducted on a WML-76 Akron abrasion testing machine. The rotate velocities of the sample wheel and the empery wheel were 76 rpm and 33 rpm, respectively, and the angle between the shafts of the two related wheels was 15°. A pressure of 26.7 N was loaded on the sample during the wearing. The experiments were conducted at a temperature of 25°C and a humidity of 65%.

RESULTS AND DISCUSSION

Characterization of HIFR agent

SEM analysis

SEM images of the microscopic morphology of IFR and hyperbranched intumescent flame-retardant (HIFR) agent are shown in Figure 1. It clearly can be seen from Figure 1(a) that IFR agent was made up of large powders. The particle size of the largest powder was about 20–30 μm .

From Figure 1(b), we can see that polymeric materials were covered over the surface of IFR agent. It

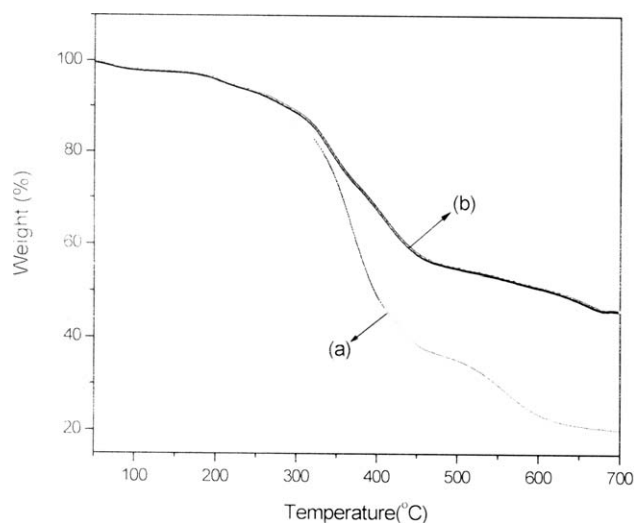


Figure 2 TGA curves of (a) IFR agent and (b) HIFR agent.

can also be seen that the diameter of the HIFR agent was about 5–10 μm . In addition, these modified IFR agents were easily separated. This indicated that hyperbranched technology was beneficial for the dispersion of aggregated powders.⁸

Thermal stability

TGA curves of IFR and HIFR agents are presented in Figure 2. The HIFR agent had an enhanced thermal behavior in comparison with that of IFR agent. With regard to the degradation of the IFR agent, which was shown in Figure 2(a), it contained three steps. Between room temperature and 250°C, the first step occurred. The second step was observed between 250 and 450°C. This was ascribed to the decomposition of oxidated materials in the residual. The third step occurred at 450–700°C followed by the formation of a stable residue about 22%.

Figure 2(b) showed TGA results of the HIFR agent, and it presented almost two reaction steps during thermal degradation. First, a pyrolysis process occurred between room temperature and 450°C. Then, a carbonaceous material relatively stable was developed in the temperature range higher than 450°C, and, finally, the degradation of this material occurred successively with a stable residue about 48%.^{9,10}

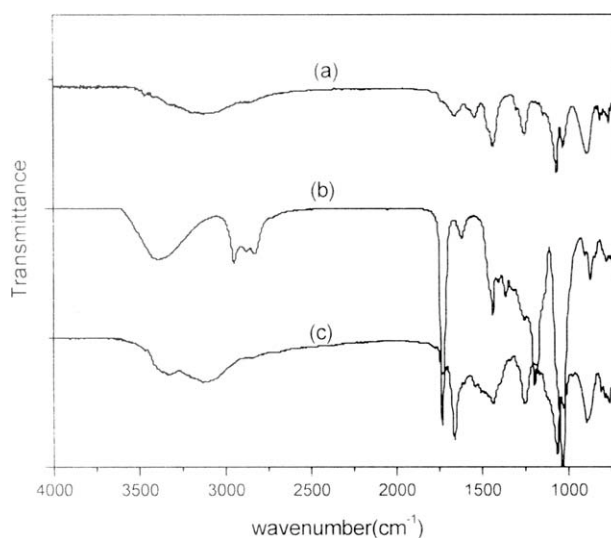
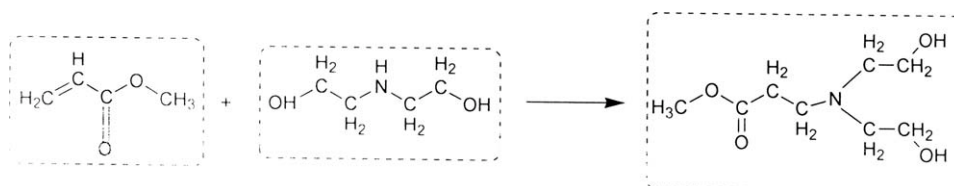


Figure 3 FTIR spectra of (a) IFR agent, (b) monomer, and (c) HIFR agent.

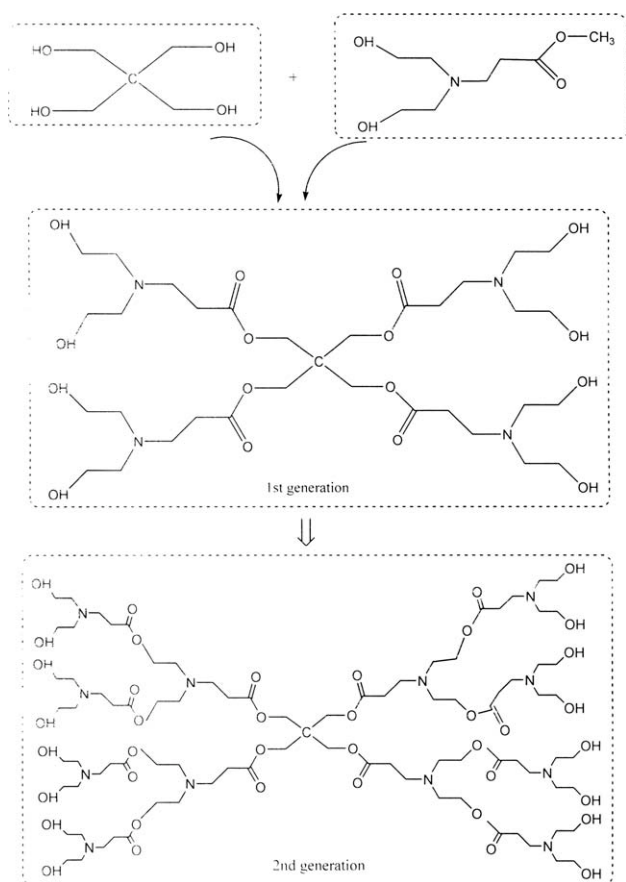
FTIR analysis

Figure 3(a–c) shows the Fourier transform infrared (FTIR) spectra of IFR agent, monomer, and the final HIFR agent, respectively. It was observed from Figure 3(a), the IFR agent, that there were two obvious absorption peaks at 2800–3000 cm^{-1} and 3000–3500 cm^{-1} , which corresponded to the stretching vibrations of C–H and –OH/N–H bonds. These were attributed to the hydroxyl, amine, methyl, or methylene groups existed in the IFR agent. The characteristic absorptions at 1500 cm^{-1} and 810 cm^{-1} resulted from the in-plane and out-of-plane bending vibrations of the aromatic structure in the triazine group of ME.^{11,12}

In the spectrum of the monomer, as shown in Figure 3(b), the 3250–3650 cm^{-1} peaks were caused by the stretching of the two hydroxyl groups. The peaks between 2800 and 3000 cm^{-1} resulted from the stretching vibration of C–H bond in the monomer structure. The appearing of strong peaks at 1760 and 1100 cm^{-1} was attributed to the –C=O and –C–O– bonds in –CH₂CH₂COOCH₃.¹³ The peak at 1270 cm^{-1} was probably assigned to the stretching vibration of C–N bond. This was due to the addition reaction between methyl acrylate and diethanolamine. The reaction for the synthesis of the monomer was shown in Scheme 1. It belonged to



Scheme 1 Chemical reaction between methyl acrylate and diethanolamine.



Scheme 2 Transesterification reaction between PER and the monomer.

Michael additional reaction.¹⁴ The H atom of —NH— in diethanolamine was very reactive. It can react with C=C in methyl acrylate to produce —N— . The methanol used here was a kind of solvent and phase transfer agent. It can accelerate the dissolution of the two reactors and improve their reaction rate.

In the spectrum of HIFR agent, except for the peaks existed in the IFR agent, there showed the presence of new peaks at 1680, 2800–3000, and 3250–3500 cm^{-1} . These were caused by corresponding stretching and bending absorptions in the monomer. The decreasing intensity of absorptions at 1760 cm^{-1} illustrated the condensation reactions between —OCH_3 in the monomer and —OH in IFR agent.

The transesterification reaction between PER and the monomer was illustrated in Scheme 2. In the process of reaction, transesterification of —OH groups with —COOCH_3 groups occurred yielding small molecules (methanol), which were continuously removed, resulting in decrease of hydroxyl value. This is in good accordance with what Wang et al.¹⁴ depicted in the synthesis of hyperbranched poly(amide-ester) polyol by a melt polycondensation technique. The aminolysis reaction between ME and the monomer was shown in Scheme 3. In this

reaction, a polycondensation reaction was occurred with the production of methanol as small molecules. Moreover, a hyperbranched polymer may be obtained from the adsorption and the later self-polycondensation occurred between APP and the monomer. This was given in Scheme 4.

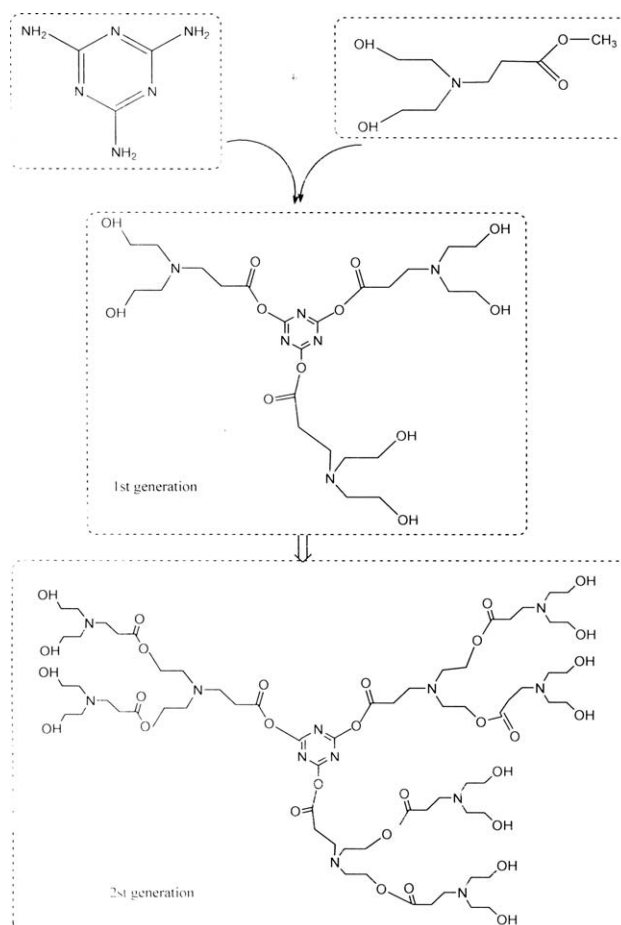
Characterization of HIFR/NR composites

Cure characteristics

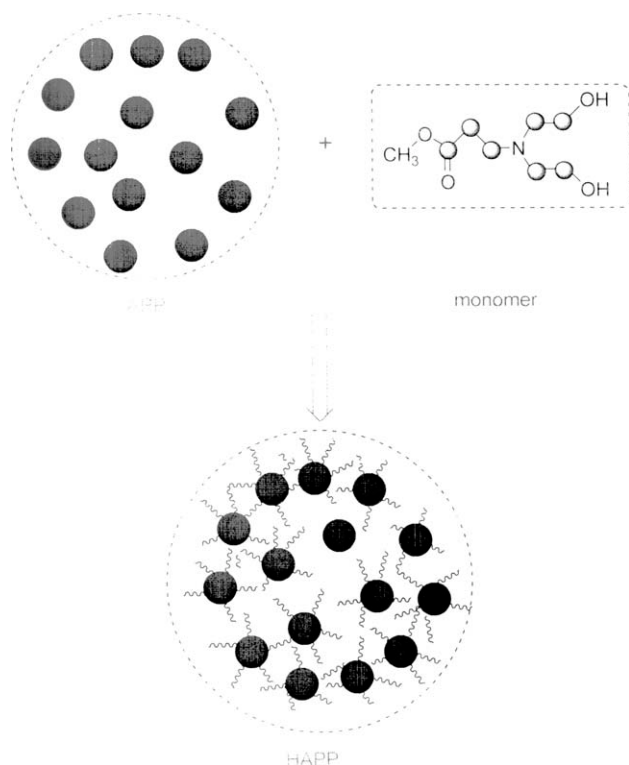
The data for the cure characteristics of the IFR/NR and Hifir/NR composites are summarized in Table II.

Scorch time is a parameter that is used to determine the safety of processing of rubber products. The longer was the scorch time, the safer was the processing. Compared to the IFR/NR composites, it can be seen that the addition of the hyperbranched intumescent flame-retardant (HIFR) agent (20–80 phr) can decrease scorch time (t_{10}) and make processing unsafe.

Technical cure time is the shortest time that is used for the rubber to reach the maximum crosslinking degree and the best mechanical properties



Scheme 3 Aminolysis reaction between ME and the monomer.



Scheme 4 Adsorption process between APP and the monomer.

during vulcanization process. The longer was the cure time, the more energy was used. It can be concluded that an energy-saving effect occurred in the vulcanization process deduced from the shortened technical cure time (t_{90}). Meanwhile, the relatively increase of minimum torque (M_L), which showed an increase of viscosity, can make HIFR/NR system not easier to process. This phenomenon may result from the “plastic effect” of the hyperbranched polymer on the HIFR/NR composites. The maximum torque (M_m) can be taken as a measurement of crosslinking density. From the results, we can see that the crosslinking density was increased after the addition of modified IFR agents. Meanwhile, the crosslinking

TABLE II
Cure Characteristic of the Different NR Systems^a

Formulation	Loading (phr)	t_{10}	t_{90}	M_L	M_m
IFR/NR	20	0.68	2.02	0.031	0.474
	40	0.67	2.06	0.025	0.395
	60	0.65	2.22	0.019	0.357
	80	0.62	2.24	0.015	0.169
HIFR/NR	20	0.62	1.38	0.023	0.926
	40	0.58	1.52	0.028	1.273
	60	0.55	1.60	0.032	1.283
	80	0.50	2.14	0.038	1.375

^a t_{10} , scorch time (min); t_{90} , technical cure time (min); M_L , minimum torque (lb. in.); M_m , maximum torque (lb. in.).

degree of HIFR/NR was increased with the amount increase of the HIFR agent, and the composite of IFR/NR showed the opposite phenomenon. This can illustrate that the hyperbranched polymer over the surface of IFR agent can increase the interfacial interaction between the IFR agent and the NR matrix and thus increased the crosslinking density of the composite.¹⁵

Tensile properties

The tensile properties of IFR/NR and HIFR/NR composites are illustrated in Figure 4. In conclusion, the HIFR-filled NR had better properties than that of IFR-filled composites.

These two kinds of composites all showed the highest tensile improvement with the addition of 20 phr amount. Compared to IFR-20/NR, the tensile strength of HIFR-20/NR was improved from 21.5 to 22.5 MPa, while the elongation at break was improved from 475 to 700%, increasing about 47%.

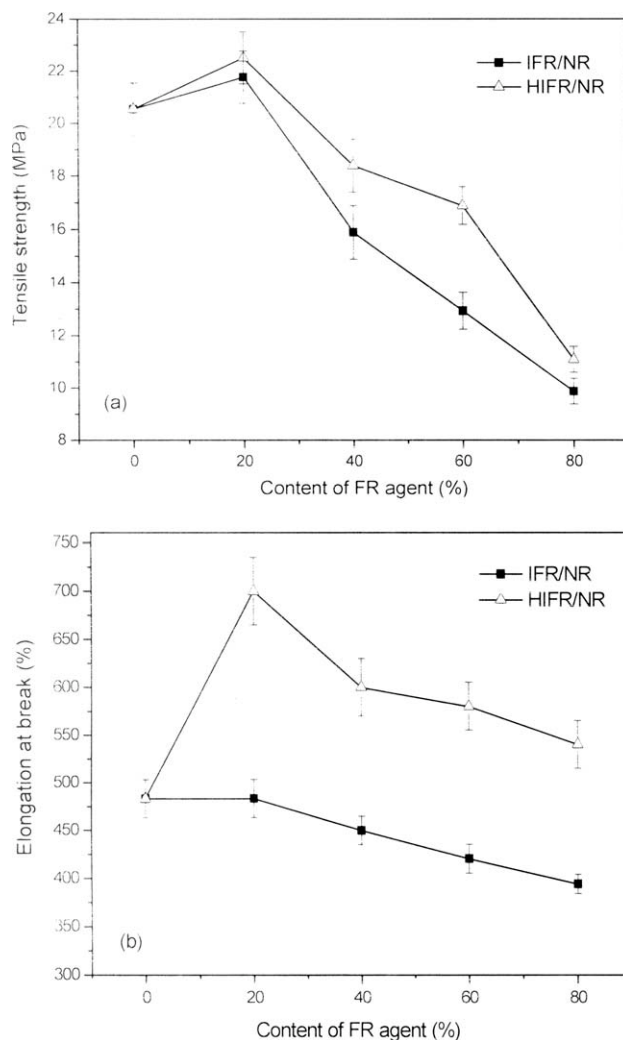


Figure 4 Tensile properties of NR composites (a) tensile strength and (b) elongation at break.

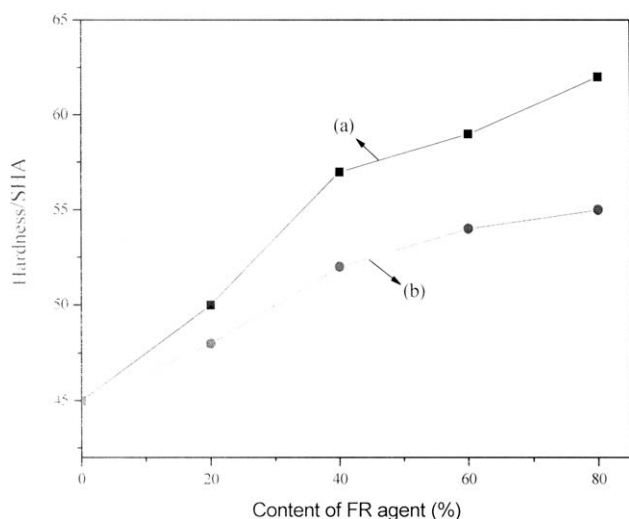


Figure 5 Shore hardness of (a) IFR/NR and (b) HIFR/NR.

When the amount of IFR or HIFR increased continuously, the tensile strength and elongation at break decreased. This was probably due to the aggregates of these fillers in the composites.¹⁶

Figure 5 shows the hardness of NR composites with IFR or HIFR agents. It can be seen that with the increasing amount of IFR agent, the hardness was increased. However, the addition of HIFR can decrease the hardness of NR composites. The HIFR agent, in some extent, may decrease the crosslinking density of NR matrix. This may be beneficial for the application of these additives in some fields that need this property.

Wear-resistant properties

Figure 6 presents the abrasion loss value of various systems with the different IFR agents. In the NR

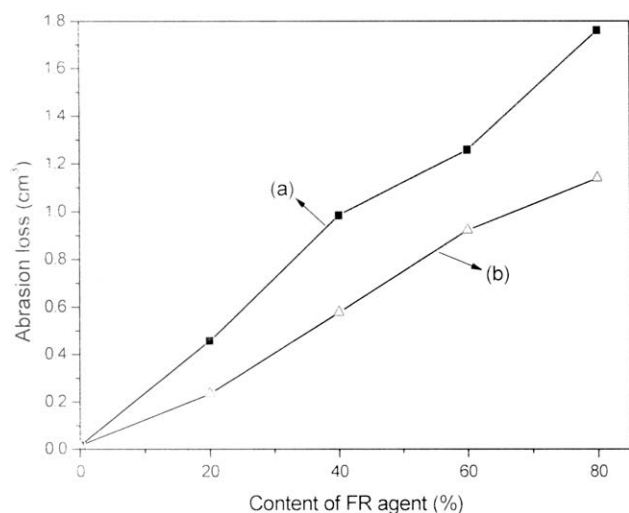


Figure 6 Abrasion loss of (a) IFR/NR and (b) HIFR/NR.

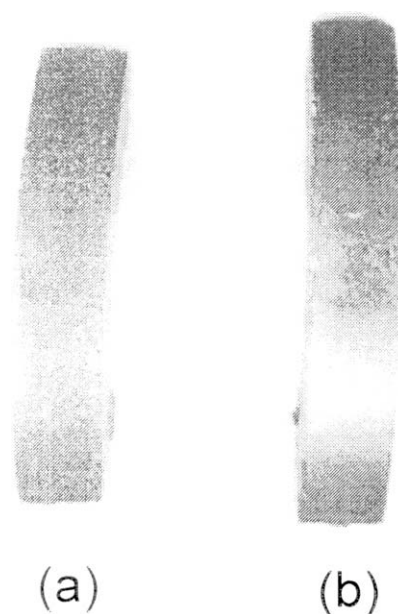


Figure 7 Worn surface photos of (a) IFR-20/NR and (b) HIFR-20/NR.

with unmodified IFR agent, the loss value showed much increase with the increase of the filler's content. The system incorporated with 20 phr of IFR agents showed the lowest abrasion loss value, that is, the best wear resistance property except for the original NR. The abrasion loss of the HIFR-20/NR was 0.234 cm³, probably 50% decrease, compared to the abrasion value 0.457 cm³ for the neat NR composite. Moreover, the abrasion loss of 80 phr of HIFR added composites was 1.140 cm³, nearly 35% decrease in comparison with that of IFR-80/NR, 1.761 cm³.¹⁷

Figure 7 shows the photos of worn surfaces of the IFR and HIFR agents' filled systems, respectively. It can be seen that the worn surface of HIFR filled system was relatively flat, while the composite containing the IFR agents accumulated holes of rubber scraps. A phenomenon can be seen during the abrasion test is that a lot of powder fell during the abrasion test of the IFR-20/NR system and that is why the worn surface of this system is relatively uneven. The reason for the flat surface appeared in the worn surface of the HIFR-20/NR composite may be resulted from the higher compatibility between the HIFR fillers and the NR matrix, which led to a higher crosslinking level and not easily worn out for this system.^{18,19}

Thermal stability

TGA study of IFR-20/NR and Hifr-20/NR systems is shown in Figure 8.

Almost two degradation steps of NR can be seen from Figure 8(a). The first step started from 260 to

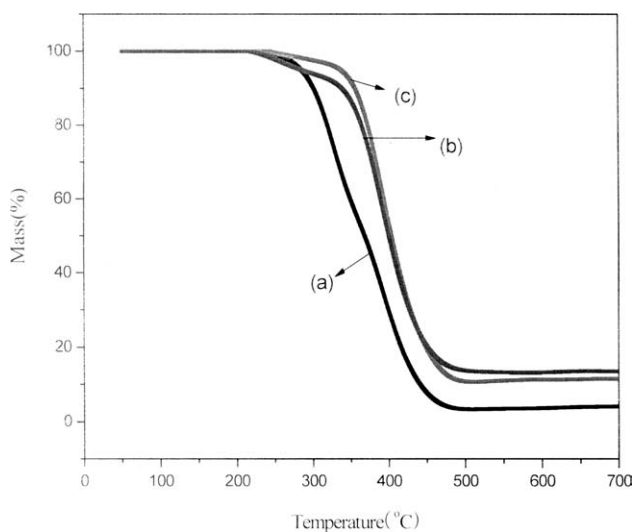


Figure 8 TGA curves of (a) NR, (b) IFR-20/NR, and (c) HIFR-20/NR.

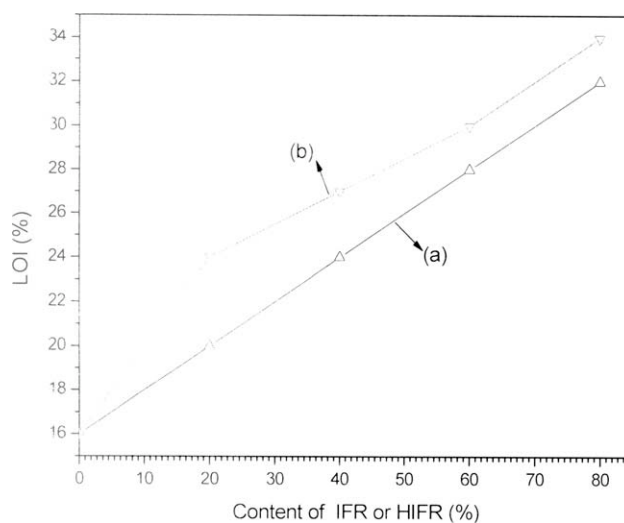


Figure 9 LOI of (a) NR/IFR and (b) NR/HIFR.

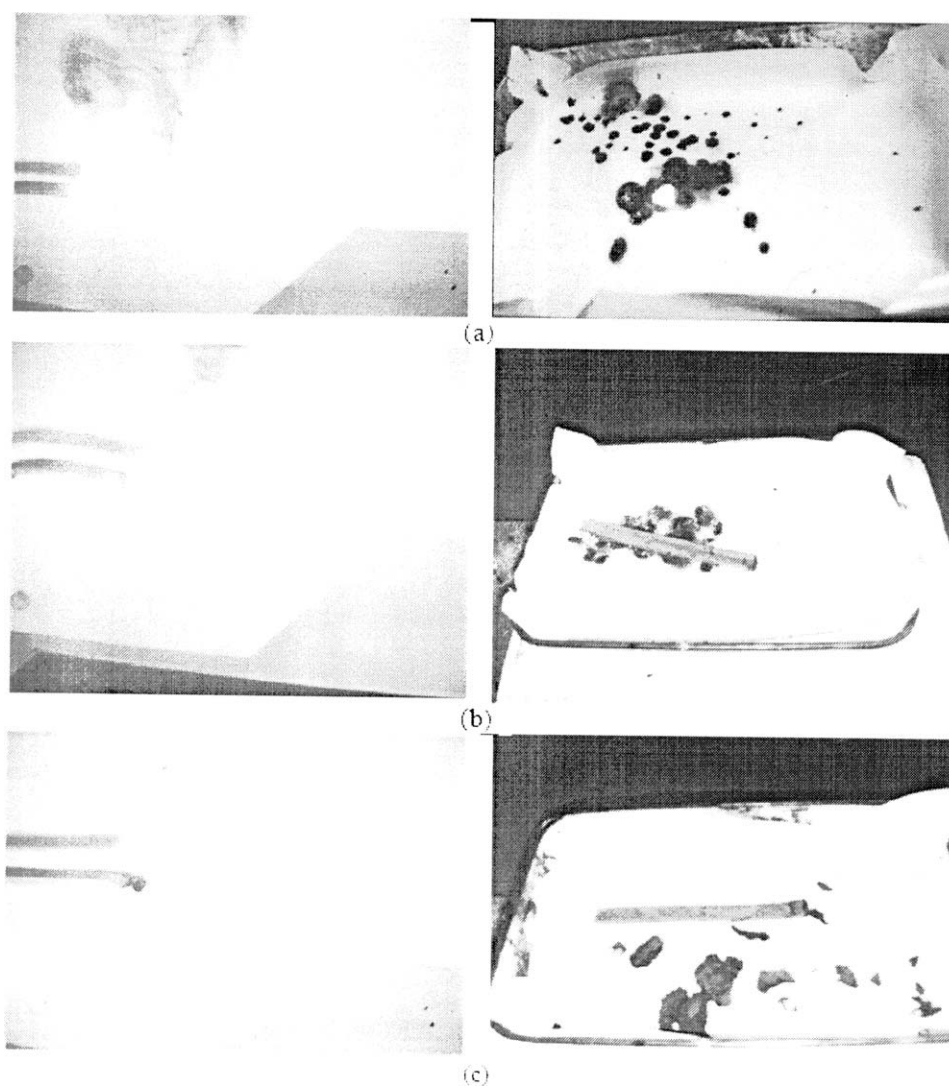


Figure 10 Horizontal burning and char layer photos of (a) NR, (b) IFR-20/NR, and (c) HIFR-20/NR.

360°C. The rate of weight loss was maximal at 360°C. The second step of degradation was observed between 360 and 470°C. It led to a residue about 4%.

The formulation of a carbonaceous material in IFR-20/NR composite occurred in two successive steps [Fig. 8(b)]. The first step, with a peak at about 320°C, may be assigned to the reaction between IFR agent and the NR system. Then, the development of intumescent material occurred by the formation of a carbonaceous material relatively stable in the temperature range 500–700°C, and finally a stable residue about 13% was left.

In the case of the formulation with HIFR agent, as shown in Figure 8(c), it presented almost the same reaction steps during thermal degradation. First, a degradation appeared between 350 and 500°C. Then, a carbonaceous material was developed and degraded in the temperature range 500–700°C, and, finally, a stable residue about 11% was remained when temperature rose higher than 500°C. Compared to that of IFR agent, the obvious difference may be ranged from 220 to 440°C, together with the residual mass. The introduction of hyperbranched polymer over the surface of IFR agent indeed improved the thermal stability of NR matrix in some temperature ranges.²⁰

Flame-retardant performance

The LOI of NR, IFR/NR, and HIFR/NR systems is shown in Figure 9. The LOI value of pure NR was very low (16.0%), which meant that NR was easily flammable. This can be seen from the photos of horizontal burning tests in Figure 10(a). By adding 20–80 phr of IFR agents into pure NR, the LOI value was increased to 32.0%. The horizontal burning photo of IFR-20/NR was shown in Figure 10(b). As can be seen, it can also be ignited. With the addition of HIFR agent into these systems, the LOI value increased to 34.0%. They showed better fire protection for NR. This was probably due to the synergistic effect between IFR agent and hyperbranched polymer. The photos, shown in Figure 10(c), were the images of horizontal burning for HIFR-20/NR composite. We can see that more carbonaceous char layers were produced compared to other two composites.²¹

CONCLUSIONS

A type of hyperbranched IFR agent was synthesized and used as flame-retardant agent for NR systems. The expected advantages for this new concept of flame-retardant agent lay in its being compatible with the NR polymeric matrix to give efficient flame-retardant and mechanical properties.

The structure and property of this HIFR agent had been examined by SEM, TGA, and FTIR. The physico-mechanical properties of NR composites loaded with different amounts of IFR and HIFR agents were also studied and compared. It was demonstrated that the NR composite filled with 20 phr of HIFR agent showed better flame-retardant, tensile, and wear-resistant properties compared to that of IFR-20/NR composite.

References

1. Menon, A. R. R. *J Fire Sci* 1997, 15, 3.
2. Wang, J. C.; Yang, S. L.; Li, G.; Jiang, J. M. *J Fire Sci* 2003, 21, 245.
3. Le Bras, M.; Bugajny, M.; Lefebvre, J. *Polym Int* 2000, 49, 1115.
4. Bourbigot, S.; Le Bras, M.; Bugajny, M. *Intumescence and Polymer Blending: an Approach for Flame Retardancy*, NIST Annual Conference, Gaithersburg, 1998.
5. Bourbigot, S.; Le Bras, M.; Delobel, R. *J Chem Soc Faraday Trans* 1996, 92, 149.
6. Camino, G.; Costa, L.; Trossarelli, L. *Polym Degrad Stab* 1984, 6, 243.
7. Tan, H. M.; Luo, Y. J.; *Hyper-branched Polymers*; Chemical Industry Press: Beijing, 2005.
8. Wang, J. C.; Yang, K.; Zheng, X. Y. *ICAFPM* 2009, II, 1019.
9. Grassie N.; Scott G. *Polymer Degradation and Stabilization*; Cambridge University Press: Cambridge, 1985.
10. Le Bras, M.; Bourbigot, S.; Le Tallec, Y.; Laureyns, J. *Polym Degrad Stab* 1997, 56, 11.
11. Ma, J.; Xu, J.; Ren, J. H. *Polymer* 2003, 44, 4619.
12. Wei, F.; Abdellatif, A. K.; Bernard, R. *Macromol Rapid Commun* 2002, 23, 703.
13. Wang, J. C.; Chen, Y. H.; Wang, J. H. *J Appl Polym Sci* 2009, 111, 658.
14. Wang, X. C.; Yuan, X. C.; Qiang, T. T.; Chen, X. *e-Polymers* 2009, 115, 1.
15. Wang, J. C.; Chen, Y.H.; Wang, J. H. *J Elast Plast* 2005, 37, 169.
16. Yeh, M. H.; Sung, H. D.; Hwang, Y. Y. *Appl Clay Sci* 2007, 38, 1.
17. Fukahori, Y. *Yamazaki Wear* 1994, 171, 195.
18. Fukahori, Y. *Yamazaki Wear* 1994, 178, 109.
19. Fukahori, Y. *Yamazaki Wear* 1995, 188, 19.
20. Wang, J. C.; Chen, Y. H. *J Fire Sci* 2005, 23, 55.
21. Dai, C. F.; Li, P. R.; Yeh, J. M. *Eur Polym J* 2008, 44, 2439.